

Cite this: *RSC Adv.*, 2017, 7, 51001

# Aqueous synthesis of highly fluorescent and stable Cu–In–S/ZnS core/shell nanocrystals for cell imaging†

Chun-Nan Zhu,<sup>ID</sup> Dong-Yun Zheng,<sup>ID</sup> Hui-Min Cao,<sup>ID</sup> Shan-Ying Zhu<sup>ID</sup> and Xiao-Jun Liu<sup>ID</sup>\*

Ternary I–III–VI nanocrystals (NCs) without toxic elements, such as Cu–In–S, are promising candidates for biolabeling and bioimaging due to their favorable biocompatibility. At present, it remains a tremendous challenge to directly synthesize high-quality Cu–In–S/ZnS core/shell NCs in aqueous solution at atmospheric pressure. Herein, a simple and reliable strategy that combines the hot-injection method and successive ion layer adsorption and reaction has been proposed to realize aqueous synthesis of fluorescent Cu–In–S/ZnS core/shell NCs. The growth of ZnS shell around Cu–In–S NCs not only improved the fluorescence quantum yield by several hundred times and to the value of 18%, but also effectively enhanced their fluorescence stability by protecting Cu<sup>+</sup> in Cu–In–S core from being oxidized to Cu<sup>2+</sup>. The prepared Cu–In–S/ZnS core/shell NCs with bright and stable fluorescence were conjugated with wheat germ agglutinin and further applied to cancer cell imaging. This strategy here should open new avenues for aqueous synthesis of high-quality nanomaterials with the core/shell structure for broad biomedical applications.

Received 14th September 2017  
Accepted 27th October 2017

DOI: 10.1039/c7ra10215a

rsc.li/rsc-advances

## 1. Introduction

Semiconductor nanocrystals (NCs), also called quantum dots (QDs), have been extensively investigated in the last two decades because of their unique optical properties, such as size-tunable fluorescence (FL), narrow emission peak, broad excitation spectrum, simultaneous excitation of multicolored QDs at a single wavelength, and excellent photostability.<sup>1–3</sup> They have served as good signal reporters for biolabeling and ideal contrast agents for cell imaging and *in vivo* cancer targeted imaging.<sup>4–7</sup> However, most of the currently used QDs contain toxic elements, such as class A elements (Cd, Pb, and Hg) and class B elements (Se, Te, and As), which will cause unfavorable biotoxicity after released from the biodegraded QDs and hinder their potential clinical applications.<sup>8–11</sup> Thus, it is highly desired to develop novel biocompatible QDs as safe probes for their widespread biological application.<sup>12–15</sup>

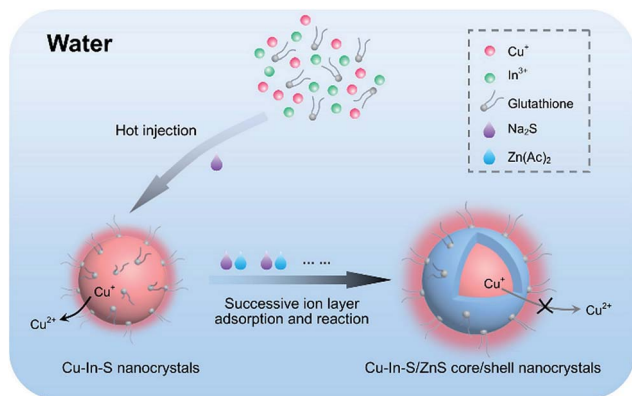
Copper indium sulfide (Cu–In–S) NCs are promising candidates as low-toxicity QDs. Pons *et al.* have demonstrated a much reduced *in vivo* local acute toxicity of CuInS<sub>2</sub>/ZnS NCs compared to CdTeSe/CdZnS QDs by studying QD-induced lymph node

inflammation.<sup>16</sup> In addition, the FL emission of Cu–In–S NCs could be tuned in the visible and near-infrared regions by tailoring the composition.<sup>17,18</sup> Due to the small lattice mismatch between ZnS and Cu–In–S of 2.2%,<sup>19,20</sup> ZnS is commonly used as the shell material to improve the quantum yields (QYs) and enhance the photostability of Cu–In–S NCs. Up to now, the main strategies for synthesizing Cu–In–S/ZnS core/shell NCs were thermal decomposition of mixed precursor solution,<sup>21–23</sup> the hot-injection strategy,<sup>24</sup> and the cation exchange reaction.<sup>25,26</sup> However, these syntheses were usually carried out at a high reaction temperature in organic solvents, which were contrary to the requirement of green and low-cost synthesis. Moreover, the obtained Cu–In–S/ZnS core/shell NCs have hydrophobic surface and need to be transferred to the aqueous phase prior to biomedical applications, which will result in a significant size increase and a decrease of FL intensity.<sup>20,27,28</sup> The subsequently developed hydrothermal approach could realize the synthesis of hydrophilic Cu–In–S NCs, and avoid additional water solubilization. But the reaction should be performed in an airtight autoclave for a long time up to 21 h.<sup>29,30</sup> In addition to be risky and time-consuming, this method is not a good choice to prepare Cu–In–S/ZnS core/shell NCs.<sup>31</sup> Compared with the above synthetic methods, directly synthesizing Cu–In–S/ZnS core/shell NCs in aqueous solution at atmospheric pressure is much simpler, greener, and cheaper. To the best of our knowledge, there are only a few reports about that, in which the FL QY and FL stability of Cu–In–S/ZnS core/shell NCs need to be comprehensively studied and further improved.<sup>32,33</sup>

Hubei Key Laboratory of Medical Information Analysis and Tumor Diagnosis & Treatment, Key Laboratory of Cognitive Science (State Ethnic Affairs Commission), College of Biomedical Engineering, South-Central University for Nationalities, Wuhan 430074, P. R. China. E-mail: liuxj@mail.scuec.edu.cn

† Electronic supplementary information (ESI) available. See DOI: 10.1039/c7ra10215a





**Scheme 1** Strategy for directly synthesizing high-quality Cu–In–S/ZnS core/shell NCs in aqueous solution at atmospheric pressure.

In this work, we have presented a simple and reliable strategy to prepare hydrophilic Cu–In–S/ZnS core/shell NCs with bright and stable FL in aqueous solution at atmospheric pressure (Scheme 1). In the two-step procedure, first Cu–In–S NCs were prepared by injecting  $\text{Na}_2\text{S}$  solution into the mixture of  $\text{CuI}$ ,  $\text{InCl}_3$ , and glutathione at  $90^\circ\text{C}$ . The resulting Cu–In–S NCs were subsequently overcoated with a ZnS shell *via* successive ion layer adsorption and reaction, which is favorable for homogeneous growth of shell precursors onto all core NCs in solution.<sup>34–37</sup> During the shell growth, the FL QY strongly increased by several hundred times and to the value of 18%, which is comparable to that of hydrophilic Cu–In–S/ZnS NCs obtained through a water solubilization process in some previous reports.<sup>28,38</sup> For the first time it was found that the ZnS shell could protect  $\text{Cu}^+$  in the Cu–In–S core from being oxidized to  $\text{Cu}^{2+}$ , and subsequently enhance their FL stability. Finally, the prepared Cu–In–S/ZnS core/shell NCs were conjugated with wheat germ agglutinin (WGA) and successfully applied to cancer cell imaging.

## 2. Experimental

### 2.1 Materials

Copper(i) iodide ( $\text{CuI}$ , 99.95% metals basis), indium(iii) chloride tetrahydrate ( $\text{InCl}_3 \cdot 4\text{H}_2\text{O}$ , 99.9% metals basis), glutathione (reduced), zinc acetate ( $\text{Zn}(\text{Ac})_2$ , 99.99%), and rhodamine 6G (R6G) were purchased from aladdin. *N*-(3-dimethylamino-propyl)-*N'*-ethylcarbodiimide hydrochloride ( $\text{EDC} \cdot \text{HCl}$ , commercial grade) was purchased from Sigma-Aldrich. 3-(4,5-Dimethyl-2-thiazolyl)-2,5-diphenyl-2-*H*-tetrazolium bromide (MTT) was purchased from Amresco. WGA and FITC-labeled WGA (FITC-WGA) were purchased from Vector. Sodium sulfide nonahydrate ( $\text{Na}_2\text{S} \cdot 9\text{H}_2\text{O}$ ), ethanol, dimethyl sulfoxide (DMSO), and sodium hydrate ( $\text{NaOH}$ ) were purchased from China National Pharmaceutical Group Corporation.

### 2.2 Synthesis of Cu–In–S NCs

For a typical synthetic reaction, 0.1 mmol of  $\text{CuI}$ , 0.2 mmol of  $\text{InCl}_3 \cdot 4\text{H}_2\text{O}$ , 1 mmol of glutathione, and 10 mL of deionized

water were loaded into a three-neck flask filled with argon. The pH of the reaction mixture was adjusted to 9.0 by stepwise addition of  $\text{NaOH}$  solution. When heated to  $90^\circ\text{C}$ , this mixture became clear and colorless. At this moment, the  $\text{Na}_2\text{S}$  solution (0.2 M, 1 mL) was swiftly injected into the reaction mixture under vigorous stirring. The color of reaction solution immediately turned from colorless to orange. Subsequently, the reaction mixture was maintained at the temperature of  $80^\circ\text{C}$  for 30 min. Then the solution was cooled down to room temperature. The products were precipitated by adding excess ethanol and centrifugation (8000 g) for 5 min. The precipitated NCs were purified *via* centrifugal filtration with centrifugal filter devices with the MWCO of 10 kDa and finally dispersed in deionized water for further characterizations.

### 2.3 *In situ* synthesis of Cu–In–S/ZnS core/shell NCs

The freshly prepared Cu–In–S NCs were directly employed to *in situ* synthesize Cu–In–S/ZnS core/shell NCs without any purification. The  $\text{Na}_2\text{S}$  solution (0.2 M, 1 mL) and the Zn precursor solution prepared by dissolving 0.2 mmol of  $\text{Zn}(\text{Ac})_2$  and 100 mg of glutathione in 1.5 mL of deionized water were added dropwise into Cu–In–S NCs. The above procedure was repeated 5 times, and each growth lasted 30 minutes. The obtained Cu–In–S/ZnS NCs were precipitated by adding excess ethanol and centrifugation (8000 g) for 5 min. The precipitate was purified *via* centrifugal filtration with centrifugal filter devices with the MWCO of 10 kDa and finally dried under vacuum into the powder for further experiments.

### 2.4 Characterization

Transmission electron microscopy (TEM) images were obtained on a JEOL JEM-2100 transmission electron microscope operated at 200 kV. Samples for TEM characterization were prepared by dropping the solution of NCs on an ultrathin-carbon-coated Ni grid and allowing the sample to dry. Powder X-ray diffraction (XRD) pattern was obtained on a Bruker D8 Advanced X-ray diffractometer (Bruker axis) using  $\text{Cu K}\alpha$  radiation (wavelength 1.5406 Å). X-ray photoelectron spectroscopy (XPS) spectra were collected on a VG Multilab 2000 X-ray photoelectron spectrometer. Fourier transform infrared (FT-IR) analysis was conducted using pressed KBr pellets with a Thermo Scientific Nicolet iS10 spectrometer. Absorption spectra in the wavelength range of 400–700 nm were recorded with a Shimadzu UV-2550 spectrophotometer. FL emission spectra were measured at the excitation wavelength of 450 nm on a PerkinElmer LS55 FL spectrophotometer. The FL QY of the sample was determined by comparison with R6G as the standard.

### 2.5 Conjugation of Cu–In–S/ZnS core/shell NCs with WGA

The purified Cu–In–S/ZnS core/shell NCs were incubated with  $\text{EDC} \cdot \text{HCl}$  and WGA at the molar ratio of 1 : 2000 : 10 at  $25^\circ\text{C}$  for 2 h. The products were purified by gel filtration on polypropylene columns (PIERCE) with the medium of Superdex 200 prep grade (GE Healthcare). Agarose gel electrophoresis of the products was performed on a DYY-6D gel electrophoresis apparatus (Beijing Liu Yi instrument factory) by using 1% (w/v)



agarose gel, and the gel was imaged on alphasystem HP system (Alpha Innotech).

## 2.6 MTT assay

Human tongue squamous cell carcinoma CAL-27 cells were purchased from China Center for Type Culture Collection (Wuhan, P. R. China). CAL-27 cells resuspended in DMEM culture medium were seeded into a 96-well plate at a density of 7000 cells per well and cultured overnight for cell attachment. Then the medium was replaced with 200  $\mu$ L of fresh medium containing different concentration of Cu-In-S/ZnS NCs (0, 5, 12.5, 25, 50, 100  $\mu$ g mL<sup>-1</sup>). After incubation for 24 h, the cells in each well were washed once with phosphate buffered saline (1  $\times$  PBS) and incubated with the mixture of 180  $\mu$ L of 1  $\times$  PBS and 20  $\mu$ L of MTT solution (5 mg mL<sup>-1</sup>) for another 4 h. Then the medium in the 96-well plate was removed, and DMSO (150  $\mu$ L) was added into each well, followed by gentle shaking for 10 min. The optical density of each well at 570 nm was recorded using a microplate spectrophotometer (MULTISKAN MK3, Thermo Scientific).

## 2.7 Cell imaging

CAL-27 cells cultured in a 6-well plate were exposed to 1  $\times$  PBS containing 5% (w/v) bovine serum albumin (BSA) for 30 min, and then incubated with FITC, FITC-WGA, Cu-In-S/ZnS NCs, or WGA-modified Cu-In-S/ZnS NCs at 37  $^{\circ}$ C for 1.5 h. Subsequently, the cells were washed with 1% (w/v) BSA. FL images were recorded with a CCD camera (Nikon DS-Ri1) mounted on an inverted FL microscope (Ti-U, Nikon, Japan), and analyzed with the Image-Pro Plus 6.0 software.

# 3. Results and discussion

## 3.1 Synthesis and characterization of Cu-In-S NCs and Cu-In-S/ZnS core/shell NCs

Fig. 1A showed the TEM image of Cu-In-S NCs, from which we can see that the Cu-In-S NCs were small well-dispersed spherical particles. Their size was measured to be  $1.8 \pm 0.4$  nm by analyzing 100 particles (Fig. 1C). The crystal structure of Cu-In-S NCs was characterized by XRD analysis, as shown in Fig. 2A (black line). The very broad diffraction peaks of Cu-In-S NCs were observed because of the small size of the particles, which can be indexed to the tetragonal crystal structure of CuInS<sub>2</sub> chalcopyrite.<sup>39</sup> Energy-dispersive X-ray (EDX) result (Fig. 2B, black line) confirmed the presence of Cu, In, and S elements in the products. It should be pointed out that the Ni element in the EDX spectrum arose from Ni grid used in the preparation of TEM sample, on which the solution of NCs was dropped. FT-IR spectrum of Cu-In-S NCs (Fig. S1 in the ESI<sup>†</sup>) demonstrated that thiol groups in glutathione have covalently bound with metal atoms on the surface of Cu-In-S NCs. Thus, it could be concluded that Cu-In-S NCs capped with glutathione have been successfully prepared.

To *in situ* coat Cu-In-S NCs with ZnS shell, successive ion layer adsorption and reaction has been employed, in which Zn precursor and S precursor were added dropwise into freshly

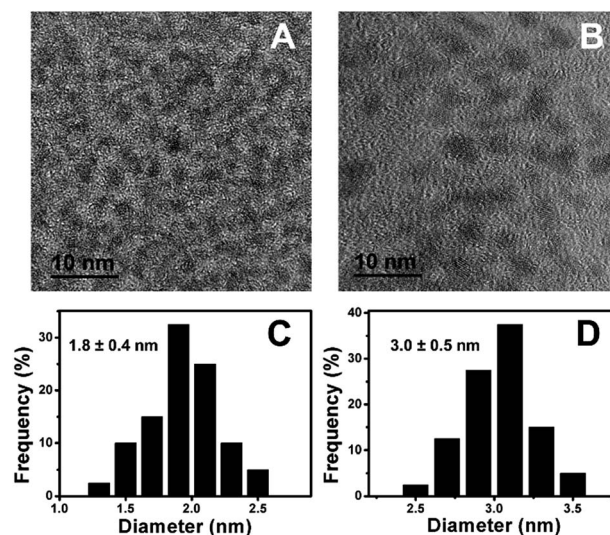


Fig. 1 TEM image (A) and the corresponding size histogram (C) of Cu-In-S NCs. TEM image (B) and the corresponding size histogram (D) of Cu-In-S/ZnS core/shell NCs.

prepared Cu-In-S NCs by turns. Firstly, the adding sequence of Zn and S precursors was studied. As shown in Fig. S2 in the ESI<sup>†</sup>, the products obtained by introducing S precursor and then Zn precursor exhibited stronger FL than that with the adding sequence of first Zn and then S precursors. It may be related to the metal-atoms-rich surface of Cu-In-S NCs with ligand of glutathione. The added S precursor could tightly bind to the metal atoms on the surface of Cu-In-S NCs as well as facilitate the subsequent Zn adsorption. Thus, the growth of ZnS shell was performed by adding S precursor and then Zn precursor into Cu-In-S NCs. When the adding of ZnS shell precursor solution was repeated five times, the FL intensity of products no longer increased (Fig. S3 in the ESI<sup>†</sup>). The as-prepared Cu-In-S/ZnS NCs underwent the characterizations of morphology, structure, and element composition. Compared with the Cu-In-S core size, the core/shell particle size of  $3.0 \pm 0.5$  nm (Fig. 1B and D) has increased by 1.2 nm, which is about the thickness of two monolayers of ZnS shell (one monolayer *ca.* 0.31 nm).<sup>40</sup> In Fig. 2A, XRD peaks of Cu-In-S/ZnS NCs shifted to higher angles toward those of the standard zinc blende ZnS. This shift of XRD peaks is usually employed to confirm the formation of core/shell structure.<sup>41,42</sup> In the EDX spectrum

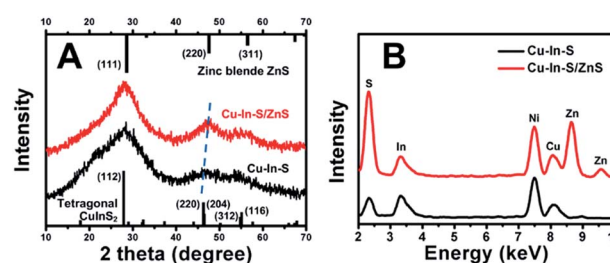


Fig. 2 XRD patterns (A) and EDX spectra (B) of Cu-In-S NCs and Cu-In-S/ZnS core/shell NCs.





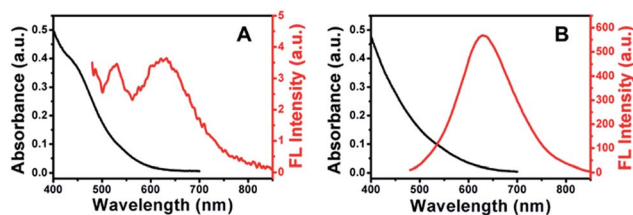


Fig. 3 Absorption and FL emission spectra of Cu-In-S NCs (A) and Cu-In-S/ZnS core/shell NCs (B).

(Fig. 2B, red line), Zn element was detected for Cu-In-S/ZnS NCs. Above all, the increase of particle size, the shift of XRD pattern to the standard ZnS peaks, and the detection of Zn element confirmed the formation of ZnS shell around the Cu-In-S NCs to obtain Cu-In-S/ZnS core/shell NCs.

### 3.2 Effect of ZnS shell on FL intensity and stability of Cu-In-S NCs

Fig. 3 showed the absorption and FL emission spectra of Cu-In-S NCs before and after the growth of ZnS shell. With the deposition of the ZnS shell upon the Cu-In-S core, the shoulder peak at around 450 nm disappeared, leaving no obvious absorption peak. In Fig. 3A, the FL of Cu-In-S core was too weak to be quantified, which may be caused by surface defects-related nonradiative recombination. The ZnS shell overcoating resulted in a slight shift of FL emission wavelength from 635 nm to 629 nm and a dramatic improvement of FL intensity by several hundred-fold (Fig. 3B), which is associated with a reduction in the nonradiative recombination dynamics due to the elimination of surface trap states by the ZnS shell. The FL QY of Cu-In-S/ZnS core/shell NCs was measured to be 18% with R6G as the reference (Fig. S4 in the ESI†), which could meet the demand of bioimaging. It was also found that the FL emission wavelength

of Cu-In-S/ZnS NCs could be tuned by varying the Cu/In raw ratios. As shown in Fig. S5 in the ESI†, when the Cu/In raw ratio was changed to 1 : 4 and to 1 : 1, the FL wavelength of Cu-In-S/ZnS NCs shifted to 608 nm and to 660 nm, respectively. With the increase of Cu/In raw ratios, the FL wavelength of Cu-In-S/ZnS NCs exhibited a red shift.

In addition to improving the FL brightness of Cu-In-S NCs, the growth of ZnS shell also has an effect on their photostability and chemical stability. So far, there are very few reports on studying the stability of hydrophilic Cu-In-S NCs directly prepared in aqueous solution. Firstly, the photostability of Cu-In-S core and Cu-In-S/ZnS core/shell NCs was examined by monitoring their FL intensity change under light irradiation. As shown in Fig. 4A, the originally weak FL of Cu-In-S NCs decrease dramatically after continuous illumination with 50 W mercury lamp, and less than 10% of FL could be retained after 90 min. However, Cu-In-S/ZnS core/shell NCs were more stable and preserved 90% of FL after irradiation for 150 min. Thus, the growth of ZnS shell has endowed Cu-In-S NCs with the property of photobleaching resistance. Besides, an interesting result in XPS analyses of freshly prepared Cu-In-S NCs and Cu-In-S/ZnS core/shell NCs has attracted our attention and promoted us to

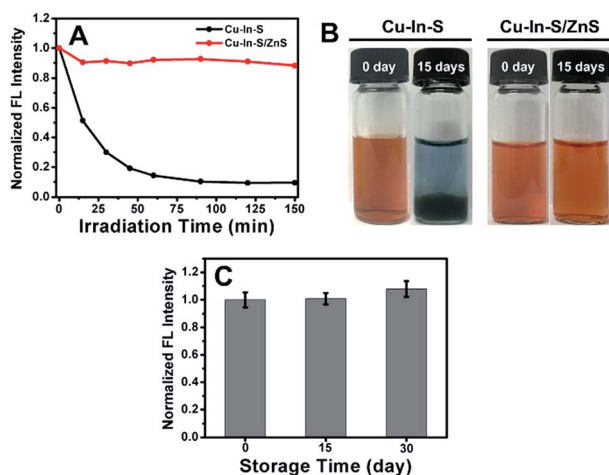


Fig. 4 (A) FL intensity change of Cu-In-S NCs and Cu-In-S/ZnS core/shell NCs after continuous illumination with 50 W mercury lamp. (B) Pictures of Cu-In-S NCs and Cu-In-S/ZnS core/shell NCs when freshly prepared and after stored at 4 °C for 15 days. (C) FL intensity change of Cu-In-S/ZnS core/shell NCs stored at 4 °C for one month.

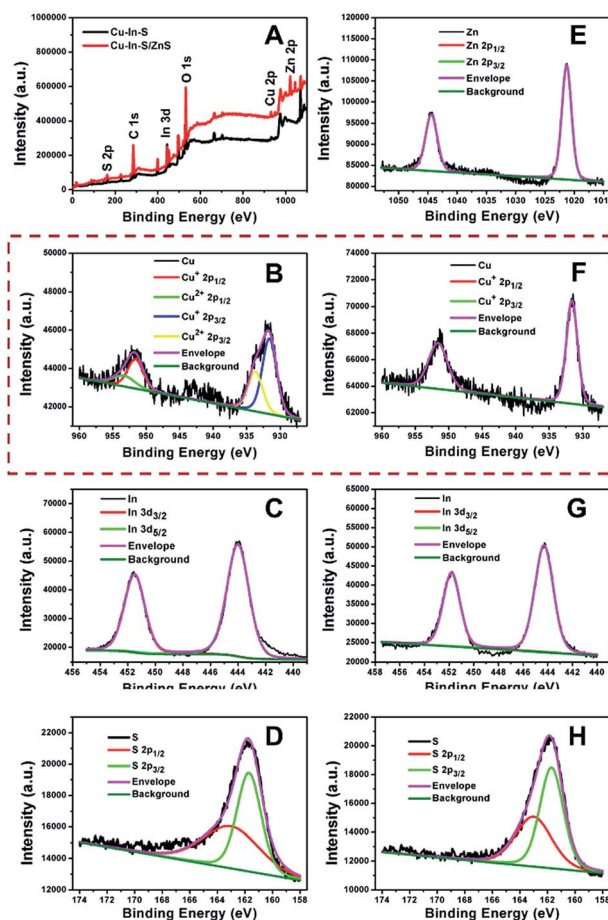


Fig. 5 (A) XPS survey spectra of Cu-In-S NCs and Cu-In-S/ZnS core/shell NCs. High-resolution XPS spectra of Cu 2p (B), In 3d (C), and S 2p (D) in Cu-In-S NCs. High-resolution XPS spectra of Zn 2p (E), Cu 2p (F), In 3d (G), and S 2p (H) in Cu-In-S/ZnS core/shell NCs.



study their chemical stability. As shown in Fig. 5B and F, the Cu element in freshly prepared Cu-In-S NCs existed in two forms of  $\text{Cu}^+$  and  $\text{Cu}^{2+}$ , while only  $\text{Cu}^+$  existed in freshly prepared Cu-In-S/ZnS core/shell NCs. According to the previous reports, the Cu element of Cu-In-S NCs is usually in the +1 valence.<sup>18,43,44</sup> Since the used Cu precursor in the synthesis was Cu(I) halides CuI, it can be deduced that  $\text{Cu}^+$  ions in the plain Cu-In-S NCs were very easily oxidized to  $\text{Cu}^{2+}$  even in the short period from synthesis, to XPS sample preparation, and finally to XPS measurement. To verify the above deduction, we continued to observe the state of the solutions containing Cu-In-S NCs or Cu-In-S/ZnS core/shell NCs. After stored at 4 °C for 15 days, the Cu-In-S solution has been layered (Fig. 4B). Lots of dark green precipitates appeared, and the supernatant turned out to be blue, which was caused by  $\text{Cu}^{2+}$  ions. Whereas Cu-In-S/ZnS core/shell NCs have maintained good dispersibility and exhibited no FL intensity change during the storage for one month (Fig. 4C). These results confirmed that the ZnS shell could protect  $\text{Cu}^+$  ions in the Cu-In-S core from being oxidized by oxidizing species such as dissolved oxygen, and subsequently enhance their chemical stability. Above all, the stability of Cu-In-S/ZnS core/shell NCs, including photostability and chemical stability, is superior to that of Cu-In-S NCs.

### 3.3 Cell imaging with Cu-In-S/ZnS core/shell NCs

In order to verify the good biocompatibility of Cu-In-S/ZnS core/shell NCs, the cytotoxicity of Cu-In-S/ZnS NCs was compared with that of CdSe/ZnS QDs by using MTT assay with CAL-27 cells as the model cell line. The cells were treated with Cu-In-S/ZnS NCs and CdSe/ZnS QDs of different concentrations from 0 to 100  $\mu\text{g mL}^{-1}$  for 24 h. As shown in Fig. 6, approximately 95% of CAL-27 cells retained viability after exposed to Cu-In-S/ZnS NCs with the concentration up to 100  $\mu\text{g mL}^{-1}$ , while the viability of CAL-27 cells significantly decreased with the increasing concentration of CdSe/ZnS QDs and only 70% of CAL-27 cells could survive at the concentration of 100  $\mu\text{g mL}^{-1}$ . The above results indicated that the cytotoxicity of Cu-In-S/ZnS NCs was much lower than that of CdSe/ZnS QDs. Thus, Cu-In-S/ZnS core/shell NCs could serve as biocompatible biomaterials.

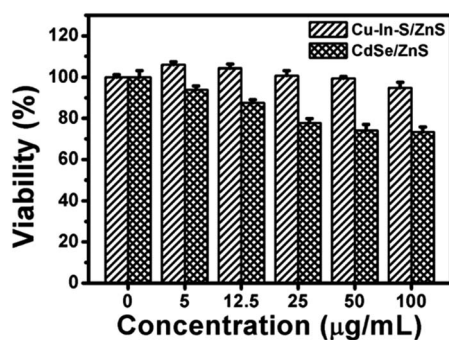


Fig. 6 MTT assays of CAL-27 cells after treated with Cu-In-S/ZnS NCs and CdSe/ZnS QDs of different concentrations from 0 to 100  $\mu\text{g mL}^{-1}$  for 24 h.

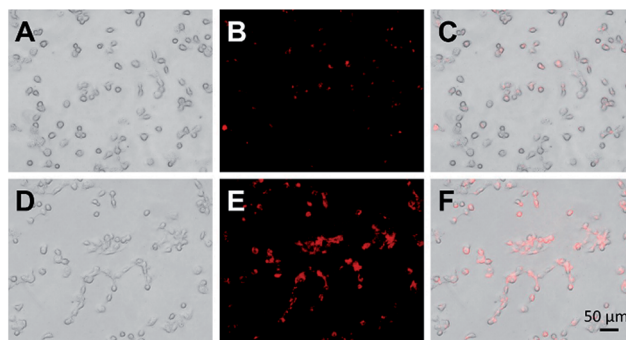


Fig. 7 Bright-field images, FL images, and the merged images of CAL-27 cells after the incubation with Cu-In-S/ZnS NCs (A–C) and WGA-modified Cu-In-S/ZnS NCs (D–F).

To determine the potential of these bright and stable Cu-In-S/ZnS NCs as optical probes for bioimaging, Cu-In-S/ZnS NCs were conjugated with WGA and then applied for FL imaging of CAL-27 cells. WGA, a kind of immunogenic lectin, could recognize some types of cancer cells by specifically binding to WGA receptors, such as *N*-acetylglucosamine (GlcNAc) and sialic acid, which are over expressed on the surface plasma membranes of cancer cells. High expression level of WGA receptors on the membrane of CAL-27 cells has been characterized by immunofluorescence assays (Fig. S6 in the ESI†). Then WGA was covalently attached to the surface of Cu-In-S/ZnS NCs *via* the interaction between amino groups and carboxyl groups to produce WGA-modified Cu-In-S/ZnS NCs. Compared to Cu-In-S/ZnS NCs, WGA-modified Cu-In-S/ZnS NCs moved more slowly in the electric field, confirming the successful conjugation of Cu-In-S/ZnS NCs with WGA (Fig. S7 in the ESI†). Fig. 7 showed the results of CAL-27 cells imaging with Cu-In-S/ZnS NCs and WGA-modified Cu-In-S/ZnS NCs. With regard to the images of Cu-In-S/ZnS NCs, only a weak red FL could be observed, indicating that only little Cu-In-S/ZnS NCs entered CAL-27 cells. However, WGA-modified Cu-In-S/ZnS NCs in CAL-27 cells exhibited strong red FL. Indeed, the presence of WGA on the surface of Cu-In-S/ZnS NCs can facilitate their cellular uptake by CAL-27 cells with high expression of WGA receptors. The results showed the great potential of Cu-In-S/ZnS NCs as biolabels for cancer cell FL imaging.

## 4. Conclusions

In summary, we have developed a simple and reliable strategy that combines the hot-injection method and successive ion layer adsorption and reaction to directly prepare highly fluorescent Cu-In-S/ZnS core/shell NCs in aqueous solution. This strategy has effectively avoided high temperatures, high pressures, and the use of organic solvents and expensive raw materials, which meets the requirement of green and low-cost synthesis. The Cu-In-S/ZnS core/shell NCs prepared by this approach showed strong FL, and their QY with value of 18% was comparable to that of hydrophilic Cu-In-S/ZnS NCs obtained through a water solubilization process. We also found for the first time that the ZnS shell could protect  $\text{Cu}^+$  in Cu-In-S NCs



from being oxidized to  $\text{Cu}^{2+}$ , and significantly enhance the FL stability of Cu–In–S NCs. The prepared Cu–In–S/ZnS core/shell NCs with bright and stable FL were conjugated with WGA and successfully applied to CAL-27 cells imaging. Moreover, this aqueous synthesis method can be extended to aqueous synthesis of other high-quality nanomaterials with the core/shell structure for broad biomedical applications.

## Conflicts of interest

There are no conflicts to declare.

## Acknowledgements

This work was supported by Wuhan Morning Light Plan of Youth Science and Technology (No. 2017050304010322), the National Nature Science Foundation of China (No. 61501526 and 61178087), and the Fundamental Research Funds for the Central Universities, South-Central University for Nationalities (No. CZQ16011, CZZ17007, and CZY14017).

## References

- W. C. W. Chan and S. M. Nie, *Science*, 1998, **281**, 2016–2018.
- I. L. Medintz, H. T. Uyeda, E. R. Goldman and H. Mattoussi, *Nat. Mater.*, 2005, **4**, 435–446.
- K. D. Wegner and N. Hildebrandt, *Chem. Soc. Rev.*, 2015, **44**, 4792–4834.
- S. L. Liu, Z. G. Wang, Z. L. Zhang and D. W. Pang, *Chem. Soc. Rev.*, 2016, **45**, 1211–1224.
- E. Z. Sun, A. A. Liu, Z. L. Zhang, S. L. Liu, Z. Q. Tian and D. W. Pang, *ACS Nano*, 2017, **11**, 4395–4406.
- Z. Y. Hong, C. Lv, A. A. Liu, S. L. Liu, E. Z. Sun, Z. L. Zhang, A. W. Lei and D. W. Pang, *ACS Nano*, 2015, **9**, 11750–11760.
- C. N. Zhu, G. Chen, Z. Q. Tian, W. Wang, W. Q. Zhong, Z. Li, Z. L. Zhang and D. W. Pang, *Small*, 2017, **13**, 1602309.
- S. J. Cho, D. Maysinger, M. Jain, B. Röder, S. Hackbarth and F. M. Winnik, *Langmuir*, 2007, **23**, 1974–1980.
- J. L. Pelley, A. S. Daar and M. A. Saner, *Toxicol. Sci.*, 2009, **112**, 276–296.
- F. M. Winnik and D. Maysinger, *Acc. Chem. Res.*, 2013, **46**, 672–680.
- M. Vinceti, E. T. Wei, C. Malagoli, M. Bergomi and G. Vivoli, *Rev. Environ. Health*, 2001, **16**, 233–251.
- Y. P. Gu, R. Cui, Z. L. Zhang, Z. X. Xie and D. W. Pang, *J. Am. Chem. Soc.*, 2012, **134**, 79–82.
- C. N. Zhu, P. Jiang, Z. L. Zhang, D. L. Zhu, Z. Q. Tian and D. W. Pang, *ACS Appl. Mater. Interfaces*, 2013, **5**, 1186–1189.
- Y. F. Wang, Y. W. Zhu, S. M. Yu and C. L. Jiang, *RSC Adv.*, 2017, **7**, 40973–40989.
- Z. T. Fan, S. H. Li, F. L. Yuan and L. Z. Fan, *RSC Adv.*, 2015, **5**, 19773–19789.
- T. Pons, E. Pic, N. Lequeux, E. Cassette, L. Bezdetnaya, F. Guillemin, F. Marchal and B. Dubertret, *ACS Nano*, 2010, **4**, 2531–2538.
- B. K. Chen, H. Z. Zhong, W. Q. Zhang, Z. A. Tan, Y. F. Li, C. R. Yu, T. Y. Zhai, Y. S. Bando, S. Y. Yang and B. S. Zou, *Adv. Funct. Mater.*, 2012, **22**, 2081–2088.
- Y. Y. Chen, S. J. Li, L. J. Huang and D. C. Pan, *Nanoscale*, 2014, **6**, 1295–1298.
- D. C. Pan, D. Weng, X. L. Wang, Q. F. Xiao, W. Chen, C. L. Xu, Z. Z. Yang and Y. F. Lu, *Chem. Commun.*, 2009, 4221–4223.
- D. W. Deng, Y. Q. Chen, J. Cao, J. M. Tian, Z. Y. Qian, S. Achilefu and Y. Q. Gu, *Chem. Mater.*, 2012, **24**, 3029–3037.
- L. Li, A. Pandey, D. J. Werder, B. P. Khanal, J. M. Pietryga and V. I. Klimov, *J. Am. Chem. Soc.*, 2011, **133**, 1176–1179.
- Y. H. Jia, H. C. Wang, Z. R. Yan, L. Deng, H. Dong, N. Ma and D. B. Sun, *RSC Adv.*, 2016, **6**, 93303–93308.
- Y. S. Kim, Y. Lee, Y. Kim, D. Kim, H. S. Choi, J. C. Park, Y. S. Nam and D. Y. Jeon, *RSC Adv.*, 2017, **7**, 10675–10682.
- R. G. Xie, M. Rutherford and X. G. Peng, *J. Am. Chem. Soc.*, 2009, **131**, 5691–5697.
- J. Park and S.-W. Kim, *J. Mater. Chem.*, 2011, **21**, 3745–3750.
- C. H. Xia, J. D. Meeldijk, H. C. Gerritsen and C. de Mello Donegá, *Chem. Mater.*, 2017, **29**, 4940–4951.
- L. Li, T. J. Daou, I. Texier, T. T. K. Chi, N. Q. Liem and P. Reiss, *Chem. Mater.*, 2009, **21**, 2422–2429.
- K. Yu, P. Ng, J. Y. Ouyang, M. B. Zaman, A. Abulrob, T. N. Baral, D. Fatehi, Z. J. Jakubek, D. Kingston, X. H. Wu, X. Y. Liu, C. Hebert, D. M. Leek and D. M. Whitfield, *ACS Appl. Mater. Interfaces*, 2013, **5**, 2870–2880.
- S. Y. Liu, H. Zhang, Y. Qiao and X. G. Su, *RSC Adv.*, 2012, **2**, 819–825.
- S. Y. Liu, F. P. Shi, X. J. Zhao, L. Chen and X. G. Su, *Biosens. Bioelectron.*, 2013, **47**, 379–384.
- R. S. Zeng, Z. G. Sun, R. A. Shen, Y. Y. Shen and X. N. Lin, *Sci. Adv. Mater.*, 2015, **7**, 1624–1628.
- Y. Y. Chen, S. J. Li, L. J. Huang and D. C. Pan, *Inorg. Chem.*, 2013, **52**, 7819–7821.
- B. T. Zhang, Y. C. Wang, C. B. Yang, S. Y. Hu, Y. Gao, Y. P. Zhang, Y. Wang, H. V. Demir, L. W. Liu and K.-T. Yong, *Phys. Chem. Chem. Phys.*, 2015, **17**, 25133–25141.
- J. J. Li, Y. A. Wang, W. Z. Guo, J. C. Keay, T. D. Mishima, M. B. Johnson and X. G. Peng, *J. Am. Chem. Soc.*, 2003, **125**, 12567–12575.
- R. S. Zeng, R. A. Shen, Y. Q. Zhao, X. S. Li, Z. G. Sun and Y. Y. Shen, *Nanotechnology*, 2014, **25**, 135602.
- R. S. Zeng, R. A. Shen, Y. Q. Zhao, Z. G. Sun, X. S. Li, J. J. Zheng, S. Cao and B. S. Zou, *CrystEngComm*, 2014, **16**, 3414–3423.
- R. S. Zeng, Z. G. Sun, S. Cao, R. A. Shen, Z. J. Liu, J. T. Long, J. J. Zheng, Y. Y. Shen and X. N. Lin, *J. Alloys Compd.*, 2015, **632**, 1–9.
- G. X. Lv, W. S. Guo, W. Zhang, T. B. Zhang, S. Y. Li, S. Z. Chen, A. S. Eltahan, D. L. Wang, Y. Q. Wang, J. C. Zhang, P. C. Wang, J. Chang and X. J. Liang, *ACS Nano*, 2016, **10**, 9637–9645.
- M. Booth, A. P. Brown, S. D. Evans and K. Critchley, *Chem. Mater.*, 2012, **24**, 2064–2070.
- B. H. Dong, L. X. Cao, G. Su and W. Liu, *Chem. Commun.*, 2010, **46**, 7331–7333.



- 41 W. N. Nan, Y. Niu, H. Y. Qin, F. Cui, Y. Yang, R. C. Lai, W. Z. Li and X. G. Peng, *J. Am. Chem. Soc.*, 2012, **134**, 19685–19693.
- 42 H. Y. Qin, Y. Niu, R. Y. Meng, X. Lin, R. C. Lai, W. Fang and X. G. Peng, *J. Am. Chem. Soc.*, 2014, **136**, 179–187.
- 43 W. W. Xiong, G. H. Yang, X. C. Wu and J. J. Zhu, *ACS Appl. Mater. Interfaces*, 2013, **5**, 8210–8216.
- 44 W. J. Yue, S. K. Han, R. X. Peng, W. Shen, H. W. Geng, F. Wu, S. W. Tao and M. T. Wang, *J. Mater. Chem.*, 2010, **20**, 7570–7578.

